

# Any-point Trajectory Modeling for Policy Learning

Chuan Wen<sup>\*1,2</sup> Xingyu Lin<sup>\*1</sup> John So<sup>\*3</sup>  
 Kai Chen<sup>6</sup> Qi Dou<sup>6</sup> Yang Gao<sup>2,4,5</sup> Pieter Abbeel<sup>1</sup>  
<sup>1</sup>UC Berkeley <sup>2</sup>IIS, Tsinghua University <sup>3</sup>Stanford University  
<sup>4</sup>Shanghai AI Laboratory <sup>5</sup>Shanghai Qi Zhi Institute <sup>6</sup>CUHK

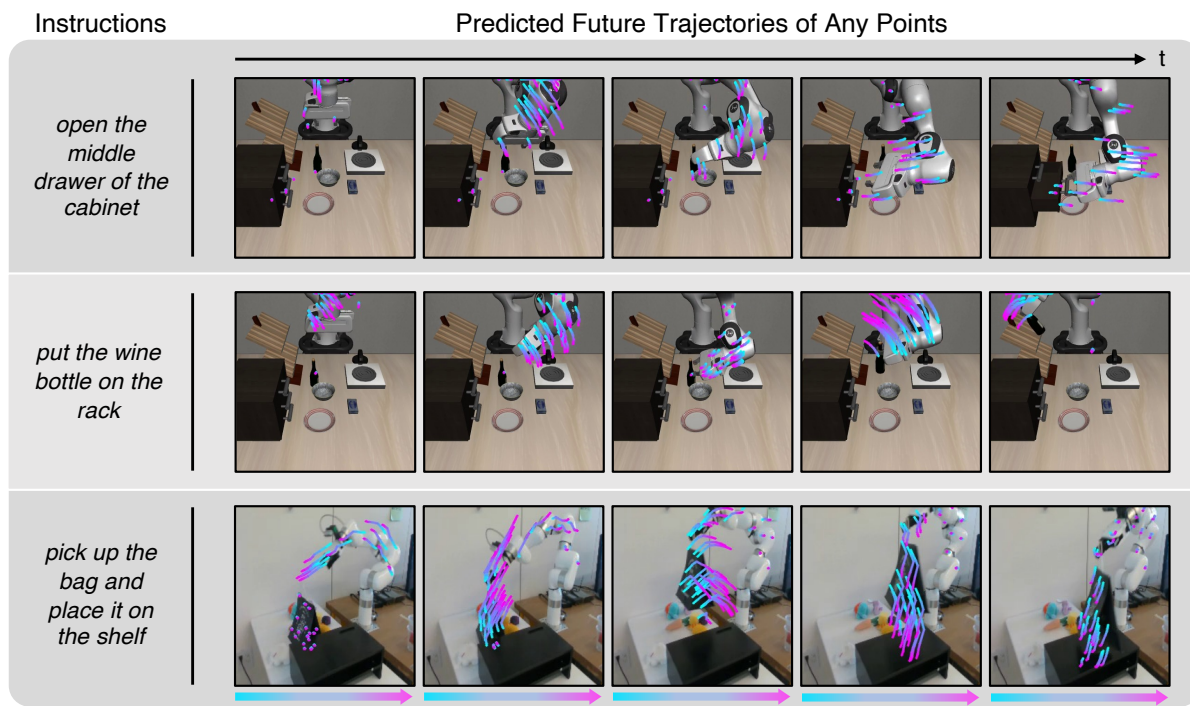


Figure 1. Given a task instruction and the initial positions of any set of points in an image frame, our **Any-point Trajectory Model (ATM)** can predict the future trajectories of these points conditioned on the task. After training the model on a video dataset, the predicted trajectories serve as effective guidance for learning visuomotor policies for a set of language-conditioned manipulation tasks.

## Abstract

*Learning from demonstration is a powerful method for teaching robots new skills, and more demonstration data often improves policy learning. However, the high cost of collecting demonstration data is a significant bottleneck. Videos, as a rich data source, contain knowledge of behaviors, physics, and semantics, but extracting control-specific information from them is challenging due to the lack of action labels. In this work, we introduce a novel framework,*

*\*First three authors contributed equally: Chuan Wen led the implementation and experiments. Xingyu Lin came up with the idea, supervised the technical development, and contributed to model debugging. John So implemented the first version of the code and the UniPi baselines.*

*Any-point Trajectory Modeling (ATM), that utilizes video demonstrations by pre-training a trajectory model to predict future trajectories of arbitrary points within a video frame. Once trained, these trajectories provide detailed control guidance, enabling the learning of robust visuomotor policies with minimal action-labeled data. Our method’s effectiveness is demonstrated across **130** simulation tasks, focusing on language-conditioned manipulation tasks. Visualizations and code are available at: <https://xingyu-lin.github.io/atm>.*

## 1. Introduction

Computer vision and natural language understanding have recently made significant advances [6, 20], largely due to the availability of large datasets. Similarly, in robotics, scaling up human demonstration data has been key for learning new skills [5, 13, 30], with a clear trend of performance improvement with larger datasets [5, 27]. However, human demonstrations, typically action-labeled trajectories collected via teleoperation devices [46, 48], are time-consuming and labor-intensive to collect. For instance, collecting 130K trajectories in [5] took 17 months, making data collection a major bottleneck in robot learning.

Videos contain knowledge about behaviors, physics, and semantics, presenting an alternative data source. However, the lack of action labels makes utilization of video data in policy learning difficult. Previous works have addressed this by using self-supervised objectives for video pre-training to learn a feature representation of the observation for policy learning [29, 37, 39]. However, a feature representation only describes the state at the current time step, largely neglecting the transition dynamics that predicts future states. To explicitly model the transition dynamics, prior works have developed video prediction models that predict future image frames from current ones [11, 12, 47]. However, learning a video prediction model for control introduces two issues. Firstly, the task of video prediction avoids any abstraction by modeling changes to every pixel, coupling the physical motion with other factors such as texture, and lighting. This coupling makes modeling difficult, often resulting in hallucinations and unrealistic future predictions [11]. Secondly, these models are computationally demanding in both training and inferencing. With limited computational resources, performance significantly declines. Moreover, the high inference cost compels these models to adopt open-loop execution [4, 11], which tends to result in less robust policies.

In this paper, we propose a novel and structured representation to bridge video pre-training and policy learning. We first represent each state as a set of points in a video frame. To model the temporal structure in videos, we learn an Any-point Trajectory Model (ATM) that takes the positions of the points in the current frame as input and outputs their future trajectories. We predict these trajectories in the camera coordinate frame to minimize the assumptions on calibrated cameras. These 2D point trajectories correspond to trajectories of particles in the 3D space and are a universal representation of the motions that can transfer to different domains and tasks. Contrasting with the video prediction approach of tracking changes in pixel intensity, our particle-based trajectory modeling offers a more faithful abstraction of the physical dynamics, naturally incorporating inductive biases like object permanence. We first pre-train the trajectory model on actionless

video datasets. After pre-training, the predicted trajectories serve as detailed guidance for the policies, functioning like subgoals. We then train trajectory-guided policies using only a minimal amount of action-labeled demonstration data. For training the ATMs, we generate self-supervised training data by leveraging recent advancements in vision models for accurate point tracking [18]. We evaluate our method on a challenging simulation benchmark comprising 130 language-conditioned manipulation tasks [25]. Our experiments demonstrate that trajectory-guided policies significantly surpass various strong baselines in video pre-training, achieving an average success rate of 63% compared to the highest success rate of 37% by previous methods, marking an improvement of over 80%. We summarize our main contributions below:

1. We propose the Any-point Trajectory Model, a simple and novel framework that bridges video pre-training to policy learning, leveraging the structured representation of particle trajectories.
2. Through extensive experiments on simulated benchmarks, we demonstrate that our method is able to effectively utilize video data in pre-training and significantly outperform various video pre-training baselines in an imitation learning setting.

## 2. Related Work

**State representation for control.** In learning end-to-end visuomotor policies, the policy is typically parameterized as a neural network that takes image observation as the input representation [5, 34, 42]. Due to the lack of inductive bias, these approaches require training on a large number of demonstration trajectories, which is expensive to collect. On the other hand, different structured representations are proposed to improve the data efficiency, such as key points [28, 32], mesh [17, 23], or neural 3D representation [22, 33]. However, prior structures often limit the policy to specific tasks. In contrast, we propose to utilize future trajectories of arbitrary points in the image as additional input to the policy, providing an effective regularization. We demonstrate its wide application to a set of 130 language-conditioned manipulation tasks. In navigation and locomotion, it is common to construct policies that are guided by the future trajectories of the robot [1, 31]. In manipulation, some works have explored flow-based guidance [14, 15, 36]. However, prior works only track task-specific points, such as the center of mass of the robot or the end-effector of the robot. Instead, our approach works with arbitrary points in different camera viewpoints, thus providing richer information in the more general settings.

**Video pre-training for control.** Videos contain rich information about behaviors and dynamics, which can help policy learning. However, video pre-training remains challenging due to the lack of action labels. One line of works

first learns an inverse dynamics model that predicts the action from two adjacent frames and then labels the videos with pseudo actions [2, 35, 40]. Once labeled, the videos can be used for behavior cloning. However, the inverse dynamics model is often trained on a limited action-labeled dataset and does not generalize well, especially for continuous actions. The imprecise action labels will later hurt policy learning. Prior works have also explored pre-train a feature representation using various self-supervised objectives [26, 29, 38], but the representation alone does not retain the temporal information in videos. More recently, learning video prediction as pre-training has shown promising results [3, 11, 12, 21, 47]. During policy learning, a video prediction model is used to generate future subgoals and then a goal-conditioned policy can be learned to reach the sub-goal. However, video prediction models often result in hallucinations and unrealistic physical motions. Furthermore, video models require extensive computation, which is an issue, especially during inference time. In contrast, our method models the trajectories of the points, naturally incorporating inductive bias like object permanence while requiring much less computation. This enables our trajectory models to be run closed-loop during policy execution. Furthermore, the trajectories provide dense guidance to the policy as a motion prior.

Finally, Vecerik et al. [41] propose to utilize any-point tracking for few-shot policy learning. This approach does not learn trajectory models from data, but instead mainly uses the tracker to perform visual servoing during test time. This design choice requires more instrumentation, such as separating the task into multiple stages, predicting the goal locations of the points for each stage, and running the tracker during inference time. In contrast, we present a much simpler framework, enabling application in more diverse settings.

### 3. Preliminary

In this paper, we aim to learn robust control policies from a small set of action-labeled demonstration trajectories. Our central goal is to leverage the more scalable, unlabeled videos as a data source for pre-training.

**Imitation from demos and videos.** To begin with, we denote the action-free video dataset as  $\mathcal{T}_o = \{(\tau_o^{(i)}, \ell^{(i)})\}_{i=1}^{N_o}$ , where  $\ell^{(i)}$  is the language instruction for the  $i^{th}$  episode and  $\tau_o^{(i)} = \{o_t^{(i)}\}_{t=1}^T$  denotes the observation-only trajectory, mainly consist of camera images. Similarly, we denote the demonstration dataset as  $\mathcal{T}_a = \{(\tau_a^{(i)}, \ell^{(i)})\}_{i=1}^{N_a}$ , where  $\tau_a^{(i)} = \{o_t^{(i)}, a_t^{(i)}\}_{t=1}^T$  is the action-labeled trajectory. During imitation learning, our goal is to learn a policy  $\pi_\theta$ , parameterized by  $\theta$  to mimic the expert behavior by the fol-

lowing behavioral cloning objective:

$$\pi_\theta^* = \arg \min_{\theta} E_{(o_t, a_t, \ell) \sim \mathcal{T}_a} \left[ \mathcal{L} \left( \pi_\theta(o_t, \ell), a_t \right) \right], \quad (1)$$

where  $\mathcal{L}$  is the loss function, which could be Mean Squared Error (MSE) or cross-entropy loss.

**Tracking Any Point (TAP).** The recent advancements in video tracking [9, 10, 43] enable us to track the trajectory of each point in video frames without external supervision. In this paper, we utilize the off-the-shelf tracker proposed in [18]. Formally, given a sequence of images from a video  $o_1, \dots, o_T$ , any one of the time steps  $\bar{t} \in [1, T]$ , and a set of points in that frame  $\{p_{\bar{t}, k}\}_{k=1}^K$ , where  $p_{\bar{t}, k} = (x, y)$  is the point coordinate in the camera frame, the task of tracking is to predict the 2D camera-frame coordinates of the corresponding points in every frame  $p_{t, k}$  where  $t = 1 \dots T$ . In this paper, we use the terms *trajectory* and *track* interchangeably to refer to a sequence of 2D coordinates of any point, denoted as  $(p_1, \dots, p_T)$ . We only model the 2D trajectories in the camera frame so that we do not have to make additional assumptions about multi-view cameras, or the availability of depth, allowing future scaling to more diverse video datasets. The tracker additionally predicts a binary visibility value  $v_{t, k}$  denoting whether the point is occluded at step  $t$ .

## 4. Method

Videos contain a great deal of prior information about the world, capturing physical dynamics, human behaviors, and semantics that are invaluable for policy learning. Beyond just learning representations from videos [26, 29, 38], we aim to learn a model from videos to predict future states for guiding a control policy. In this way, we can essentially decompose the visuomotor policy learning challenge into two parts. The first part is learning what to do next by generating future states as concrete *sub-goals*, which is learned purely from videos. The second part is learning to predict control actions to follow the sub-goals, which require much less data to train compared to learning policies end-to-end. With sufficient video pre-training, we will be able to learn generalizable policies even from limited action-labeled trajectories. Prior works [4, 11, 21] have predominantly relied on pixel-level future frame prediction as video pre-training. While video prediction is resource-intensive during both training and inference stages, its focus on reconstructing pixel-level details, which are often extraneous to policy learning, can adversely affect the efficiency of subsequent policy learning.

We propose **Any-point Trajectory Modeling (ATM)**. As illustrated in Figure 2, ATM learns to predict future point trajectories in a video frame as the pre-training, then uses the predicted trajectories to guide policy learning. Our proposed method will be comprehensively detailed in this sec-

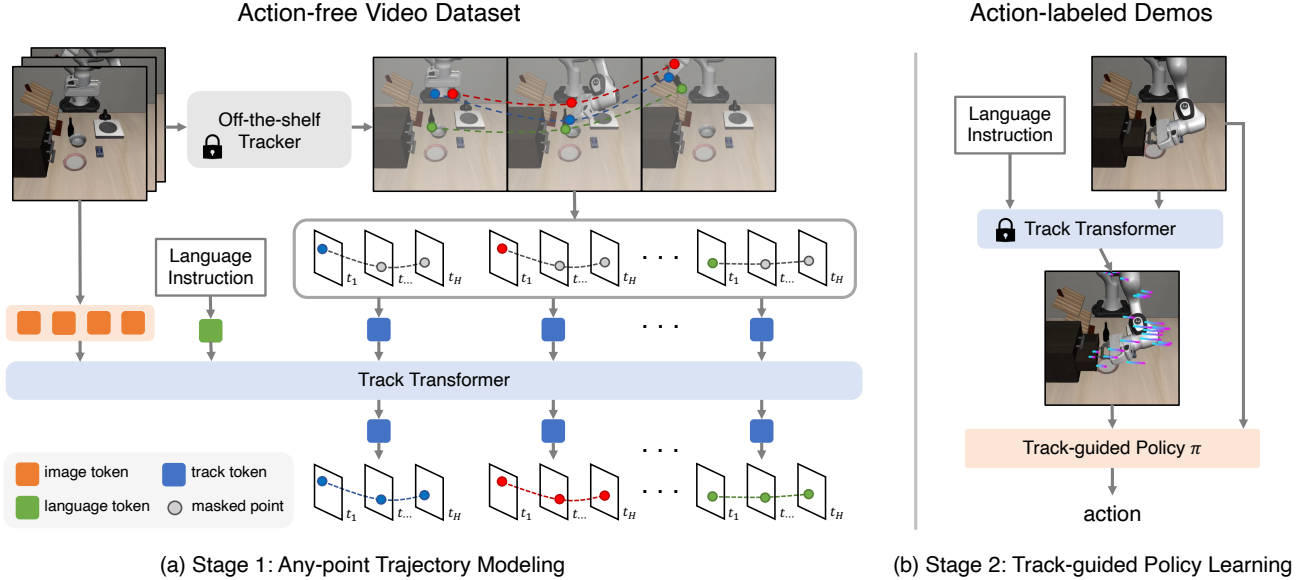


Figure 2. Overview of our framework. (a) In the first stage, given an action-free video dataset, we first sample 2D points on one video frame and track their trajectories throughout the video using a pre-trained tracker. We then train a track transformer to predict future point trajectories given the current image observation, the language instruction, and the initial positions of the points. For the transformer input, we replace the future point positions with masked values. (2) In the second stage, we learn a track-guided policy to predict the control actions. Guidance from the predicted track enables us to learn robust policies from only a few action-labeled demonstrations.

tion: In Sec. 4.1, we first describe how to learn a point trajectory prediction model from an action-free video dataset  $\mathcal{T}_o$ . Then in Sec. 4.2, we outline how we utilize the pre-trained track prediction model to learn a track-guided policy from a limited action-labeled trajectory datasets  $\mathcal{T}_a$ .

#### 4.1. Trajectory Modeling from Video Datasets

Our goal is to pre-train a model from videos that forecasts the future point trajectories in a frame. More formally, given an image observation  $o_t$  at timestep  $t$ , any set of 2D query points on the image frame  $\mathbf{p}_t = \{p_{t,k}\}_{k=1}^K$ , and a language instruction  $\ell$ , we learn a model  $\mathbf{p}_{t:t+H} = \tau_\theta(o_t, \mathbf{p}_t, \ell)$  that predicts the coordinates of the query points in the future  $H$  steps in the camera frame, where  $\mathbf{p}_{t:t+H} \in \mathbb{R}^{H \times K \times 2}$ . To model the tracks, we propose a **track transformer** and illustrate the architecture in Figure 2 (a).

**Self-supervised Track Annotation.** Initially, we generate point trajectories from action-free videos for trajectory modeling pre-training. As described in Sec. 3, we employ a vision tracker to pre-process videos and generate a tracking dataset. For each video, we randomly sample a time step  $\bar{t}$  and then randomly sample points on this frame and generate their tracks by running the tracker. However, for a static camera, most of the points that are sampled randomly will be in the background, thus providing little information when training our track transformer. To address this, we

adopt a heuristic solution to filter out these static points: we first sample a grid of  $n \times n$  on frame  $\bar{t}$  and track the grid of points across the whole of the video to obtain an initial set of tracks  $\tau \in \mathbb{R}^{n^2 \times T \times 2}$ . Subsequently, we filter points that have not moved during the video by thresholding the variance of the point positions over time. In the final step, we resample points around the filtered locations and finally generate their positions using the tracker.

**Multimodal Track Modeling.** We formalize the future forecasting problem as a multi-modal masked prediction problem: we aim to predict the future positions of each point, conditioned on its current position, the current image observation, and a language instruction of the task. We first encode different modalities into a shared embedding space, each represented by a few tokens. For the tracks, we mask out the future positions of all points before encoding and then separately encode each point into one token. For the language instruction, we use a pre-trained BERT [8] encoder. For the images, we split them into image patches and randomly masked out 50% of the patches. We then pass all tokens through a large transformer model. Finally, we decode the track tokens into future trajectories of the corresponding points. Additionally, we reconstruct the image patches from the corresponding tokens following He et al. [16] as an auxiliary task, which we find useful for more complex tasks. Through this pre-training process, our track

transformer learns the motion prior of particles within the video frames.

## 4.2. Track-guided Policy Learning

After training a track transformer to predict future tracks based on observations, we can then learn policies guided by these predicted trajectories.

**Arbitrary Points Tracking.** While in training, we can filter out points without large movements to accelerate training, such a heuristic requires knowing the future positions of each point, which can be expensive to compute at test time. Instead, we find it sufficient to simply use a fixed set of 32 points on a grid for the policy. This sampling method avoids the potential complexities of learning key points or finding points to track [41] and works well in practice. ATM is permutation invariant to the input set of points, and we also find ATM to be robust to the distribution of the points, allowing us to use a different point sampling scheme from training for policy learning.

**Track-guided Policy Learning.** A track-guided policy  $\pi(a_t|o_t, \mathbf{p}_{t:t+H})$  takes input the current observation  $o_t$  and the predicted tracks  $\mathbf{p}_{t:t+H}$  and predict the actions. A simplified illustration of our policy architecture is shown in Figure 3. Our transformer policy architecture follows the architecture in prior works [19, 25]. Although the predicted tracks alone already provide rich information to predict the actions, we still incorporate contextual image observations into our policy so that no information is lost, as suggested in prior works [24]. We incorporate the track tokens both before and after fusion with the image tokens (early fusion and late fusion) to ensure that the guiding information from tracks can be effectively integrated. Surprisingly, as the tracks already provide the fine-grained subgoals, we find that the policy no longer needs language instruction at this stage as task specification. Essentially, the provided tracks have reduced the difficult policy learning problems into a much easier sub-goal following problems, reducing the policy into an inverse dynamics model. Our track-guided policy is trained with MSE loss. A detailed architecture diagram and hyperparameters are available in the appendix.

## 5. Experiments

We conduct comprehensive experiments on 130 language-conditioned robotic manipulation tasks, to demonstrate the effectiveness of modeling point trajectories as video pre-training. Through extensive experiments, we aim to compare our method with strong baselines that pre-train from actionless videos. Additionally, we aim to demonstrate the importance of using a structured representation over RGB

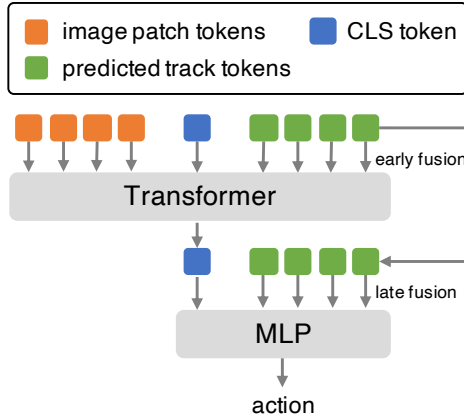


Figure 3. A visual illustration of the architecture of the track-guided policy. Given the current observation and the predicted tracks from the frozen pre-trained track transformer, we train a track-guided policy from a limited demonstration dataset.

images. Finally, we aim to show the importance of various architectural design choices and provide visualizations to validate our claims.

### 5.1. Experiment Setup

**Environments.** We compare with baselines on over one hundred language-conditioned manipulation tasks in the LIBERO benchmark [25]. The benchmark is subdivided into five suites, LIBERO-Spatial, LIBERO-Object, LIBERO-Goal, LIBERO-Long, and LIBERO-90. Each suite focuses on different challenges in learning manipulation policies, such as the ability to reason about different scene layouts, object categories, task specifications, and long-horizon tasks. Each suite has 10 tasks, except LIBERO-90 which contains 90 tasks. Specifically, LIBERO-Spatial has tasks with the same objects but different layouts; LIBERO-Object has tasks with the same layouts but different objects; LIBERO-Goal has tasks with the same object categories and spatial layouts, but different goals; LIBERO-Long has tasks with diverse object categories and layouts, and long-horizon task goals; LIBERO-90 has extremely diverse object categories, layouts and task goals.

Across all suites, each task contains 50 demonstrations, including camera images as the observation. We only utilize the image observations for video pre-training. After video pre-training, all methods use 20% of the action-labeled demonstration trajectories (i.e., 10 demonstration trajectories for each task) to train behavioral cloning policies. The policies take RGB images from a third-person camera and a wrist camera, together with gripper and joint states as observations. As each task is specified by a language instruction, we use the pre-trained BERT network to obtain a task

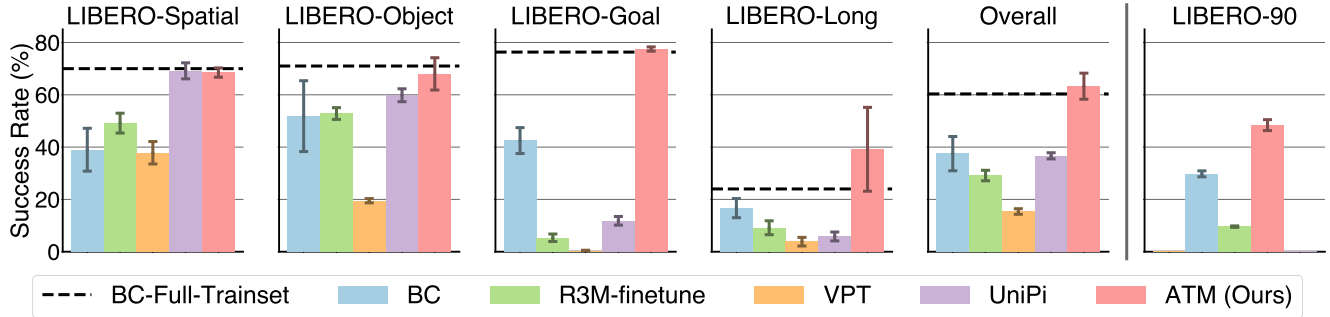


Figure 4. Task successes on the LIBERO benchmark. Our method significantly outperforms various baselines and approach the performance of BC trained on five times more demonstration data. We did not compare with UniPi on LIBERO-90 due to its high computation cost. The *Overall* success rates are computed over LIBERO- $\{\text{Spatial, Object, Goal, Long}\}$ .

embedding [8]. In our experiments, the image resolution is  $128 \times 128$  and the action space is 7-dimension, representing the translation, rotation, and aperture of the end-effector.

Policy performance is measured by success rate: a score of 1 for complete task fulfillment, and 0 otherwise. Each policy is evaluated on 20 test rollout trajectories per task, and the success rates for each suite are averaged across all tasks. We report the mean and standard deviation of each suite’s average success rate across 3 seeds.

## 5.2. Baselines

Our work primarily concentrates on leveraging unlabeled video data to boost policy learning. In this context, we compare our method against four distinctive baselines for video pre-training:

1. **BC** denotes the vanilla behavioral cloning method which trains a policy exclusively using the limited action-labeled expert demonstrations. This method does not leverage the priors from videos.
2. **R3M-finetune** [29] uses a contrastive learning objective for learning representation that aligns video and language with a combination of time contrastive losses,  $L_1$  regularization, and language consistency losses. We adopt the publicly released Ego4D pre-trained weights and fine-tune the weights on our in-domain video dataset  $\mathcal{T}_o$ , to initialize the behavioral cloning policy’s visual encoder. During policy training, we also further fine-tune the R3M backbone with the behavioral cloning loss. While this method captures priors from action-free videos through representation learning, the visual representation lacks knowledge about the transition dynamics critical to decision-making.
3. **VPT** [2] first trains an inverse dynamic model from expert demonstrations on the video dataset  $\mathcal{T}_a$  and then uses it to predict action labels for the video dataset. With these pseudo-labels, a policy is trained through behavioral cloning. This method requires the inverse dynamics model to be robust to a wide distribution of input obser-

vation, which can be difficult to learn from the limited demonstrations.

4. **UniPi** [4, 11, 21] trains a text-conditioned video diffusion model to generate a temporally fine-grained video plan from an initial frame and a language instruction. During policy learning, UniPi trains an inverse dynamic model with action-labeled data. We base our implementation off of the UniPi implementation in Ko et al. [21]. While both UniPi and ATM leverage a policy conditioned on future subgoals, a trajectory representation decouples motion from other pixel-based information and makes policy learning much easier. Please see the Appendix where we perform comprehensive comparisons on different variations of UniPi.

## 5.3. Results

We present the main results in Figure 4. We see that by bridging the video data and policy learning with the structured representation of point trajectories, ATM (our method) significantly surpasses various strong baselines in video pre-training, achieving an average success rate of 63% compared to the highest success rate of 37% by previous methods, marking an improvement of over 80%.

Compared with the vanilla BC baseline, ATM exhibits superior performance in all suites, showing significant knowledge transfer from the video dataset. R3M-finetune performs significantly worse than our method across all the suites, demonstrating the importance of explicitly modeling the transition dynamics for policy learning. As a representative paradigm for learning from videos, VPT exhibits the worst performance. We empirically observed that the pseudo-action labels predicted by VPT generally show higher errors than what can be learned from an end-to-end policy. Training with these imprecise action labels will further amplify the errors. We see that learning a good inverse dynamics model from limited demonstration data and for continuous action spaces can be challenging.

While the UniPi baseline performs similarly to ATM

on the LIBERO-Spatial and LIBERO-Object, ATM significantly outperforms UniPi on LIBERO-Goal and LIBERO-Long, which requires understanding the tasks precisely and performing complex long-horizon tasks. Both UniPi and ATM share similar algorithmic components. While UniPi learns to propose future image observation as sub-goals, ATM uses future point trajectories as sub-goals. This comparison highlights the benefits of using a structured, trajectory sub-goal compared to an image goal.

From these comparisons, we found that ATM excels at the LIBERO-Spatial, LIBERO-Long, and LIBERO-90 suites. These tasks contain more diverse tasks and long-horizon tasks. ATM’s superior performance on these more challenging tasks shows its scalability to challenging robotics tasks and the importance of decoupling motions from pixel-based features.

#### 5.4. Analysis

Next, we conduct a series of analysis experiments on LIBERO-Spatial, LIBERO-Object, LIBERO-Goal, and LIBERO-Long (omitting LIBERO-90 to save training and evaluation time) to explore the effect of the number of training demos and length of predicted tracks and ablate the components of track transformer and policy architectures.

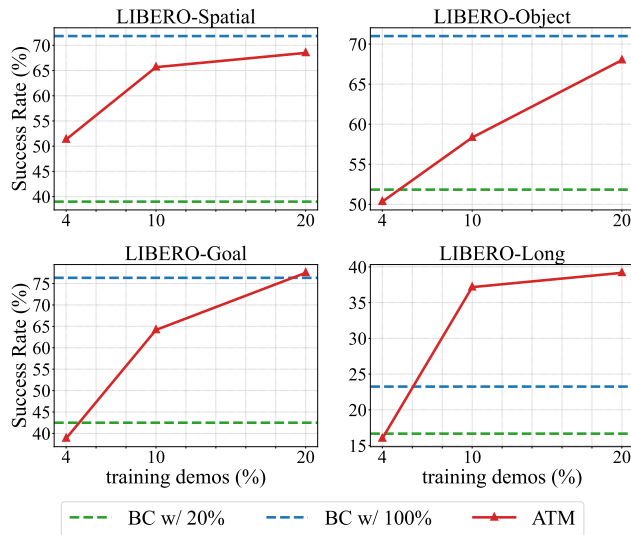


Figure 5. Success rate of our policy trained with 4%, 10% and 20% action-labeled demos. Our policy trained with only 4% demos performs comparable to BC baseline with 20% demos on LIBERO-Spatial, Object and GOAL, and even better on LIBERO-Spatial. When trained on 20% demos, our performance approaches BC with all training data.

**Effect of the number of expert demos.** As shown in Figure 5, we evaluated the performance of ATM with various numbers of action labelled demonstrations. In our default setting, as described in Section 5.3, we used 20%

of the LIBERO dataset as action-labeled demonstrations. We also reduced the training set further to 10% and 4%, which are equivalent to 5 and 2 demonstrations per task, respectively. The results show a decline in success rates with fewer demonstrations, underscoring the importance of adequate data for training effective low-level control policies. However, ATM’s performance with only 4% training demonstrations is comparable to BC w/ 20% on LIBERO-Object, Goal, and Long, and it is even significantly better on LIBERO-Spatial. Moreover, the performance of ATM trained with 20% of the demonstrations nearly matches that of BC trained with the entire dataset on three short-horizon suites. For long-horizon tasks in LIBERO-Long, enhanced by the fine-grained subgoals provided by predicted tracks, ATM with 20% demonstrations significantly outperforms BC w/ 100%. This indicates that pre-training on an action-free video dataset using our any-point trajectory modeling framework notably improves the sample efficiency of policy learning.

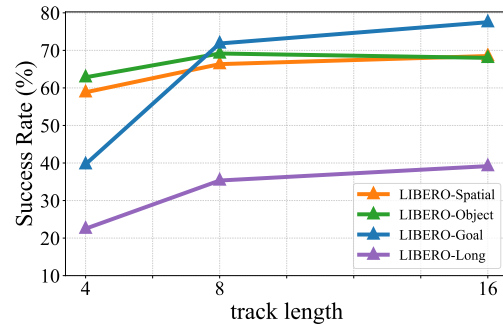


Figure 6. Success rate with different track lengths. In general, longer tracks correspond to higher success rates, except for LIBERO-Object which performs best with 8-step tracks.

**Effect of track length.** The track length of our pre-trained track transformer is 16 and we utilize all 16 points of each track by default as input for our policy. In this experiment, we investigate the effect of track length of our policy input, by training our policy with the predicted tracks truncated into 4, 8, and 16 steps. The results in Figure 6 demonstrate that longer tracks result in higher success rates in general, except LIBERO-Object where track length = 8 yields the best performance. In particular, reducing track length leads to larger performance drops on LIBERO-Goal and LIBERO-Long. These tasks require a comprehensive understanding of the task goal. Longer tracks provide more detailed and specific subgoals for each task, which is crucial for guiding the agent’s movements and actions in subsequent stage. Conversely, for LIBERO-Object which emphasizes precision operations over understanding of the task goal, a policy with a length of 16 underperforms slightly compared to the model with a length of 8. We hypothesize that the longer tracks might interfere with the learning of

Table 1. Ablation study on image masking of track transformer, where “w/o image masking” represents that we do not mask out image patches during track transformer training and “w/ image masking” means we randomly mask 50% patches. We can see that mask image modeling in track transformer improves the policy performance.

Image Mask Ratio	Spatial	Object	Goal	Long
w/o image masking	69.17 ± 6.38	65.00 ± 3.89	74.33 ± 3.66	30.83 ± 11.43
w/ image masking (default)	68.50 ± 1.78	68.00 ± 6.18	77.83 ± 0.82	39.33 ± 15.80

Table 2. Ablation study on the policy architecture. We explore the effect of the tracks fed into the policy in two positions: spatial transformer (early fusion) and MLP head (late fusion), as illustrated in Figure 9.

early fusion	late fusion	Spatial	Object	Goal	Long
✓	✗	44.67 ± 1.84	56.67 ± 3.09	5.33 ± 0.24	22.33 ± 4.94
✗	✓	65.50 ± 3.89	60.00 ± 1.47	72.83 ± 4.73	42.76 ± 14.62
✓	✓	68.50 ± 1.78	68.00 ± 6.18	77.83 ± 0.82	39.33 ± 15.80

inverse dynamics due to noise. This also supports our approach of employing tracks both as subgoal conditions and in leveraging the nature of inverse dynamics.

**Effect of image masking in track transformer.** we investigate the effects of image patch masking within our track transformer on policy performance. We conduct an ablation study by nullifying the image patch masking (setting the masking ratio to 0%) and comparing it against our standard configuration (50% masking ratio). In Table 1, the results reveal a slight decline in policy performance across three out of four test suites (LIBERO-Object, LIBERO-Goal, and LIBERO-Long) when image masking is omitted. This outcome suggests that reconstructing masked image patches is a good auxiliary task for the track transformer.

**Effect of early and late fusion in policy architecture.** As shown in Figure 3 and Figure 9, the predicted tracks are fed into the policy from two places: spatial transformer (early fusion) and MLP head (late fusion). We conduct ablation studies by removing these two track inputs to illustrate the effect of them respectively. The results are shown in Table 2. We can see that removing the late fusion leads to the most significant performance drop; on LIBERO-Goal, *w/ only early fusion* performs similarly to other baselines, whereas late fusion performs marginally worse than our full method. This reinforces the strength of tracks of specifying subgoals, and suggests that unencoded tracks themselves are easily interpretable, enabling goal-following behavior.

### 5.5. Visualization

**Attention map visualization.** To demonstrate how tracks guide the policy, we visualize the attention maps between the spatial CLS token and RGB tokens in spatial transformer of BC and our method. Figure 7 demonstrates that our method effectively focuses on the relevant spatial regions, as specified by the textual instructions. Specifically,

it attends to the cream cheese, bowl, and wine bottle in the respective example tasks, while BC is usually distracted by the irrelevant regions, highlighting the superior capability of the tracks as better task prompts.

**Tracks prediction visualization.** To qualitatively illustrate the effectiveness of our track transformer, we visualized the predicted tracks during an online rollout. As depicted in Figure 8, these tracks consistently align with the provided task-specific language instructions, maintaining directional accuracy throughout. Moreover, the predicted tracks effectively decompose the abstract textual instructions into detailed subgoals. This decomposition, combined with the policy’s precise lane adherence, contributes significantly to its promising performance.

## 6. Conclusions

In this work, we present an any-point trajectory modeling framework as video pre-training that effectively learns behaviors and dynamics from action-free video datasets. After pre-training, by learning a track-guided policy, we demonstrate significant improvements over prior state-of-the-art approaches for video pre-training followed by policy learning. We show that a particle-based representation is interpretable, structured, and naturally incorporates physical inductive biases such as object permanence. We hope our works will open doors to more exciting directions in learning from the rich source of video data for robotics applications.

## 7. Limitations

One limitation of our current work is that we only pre-train on in-domain videos, limiting the type of variations our track-guided policy could generalize to. In the future, we



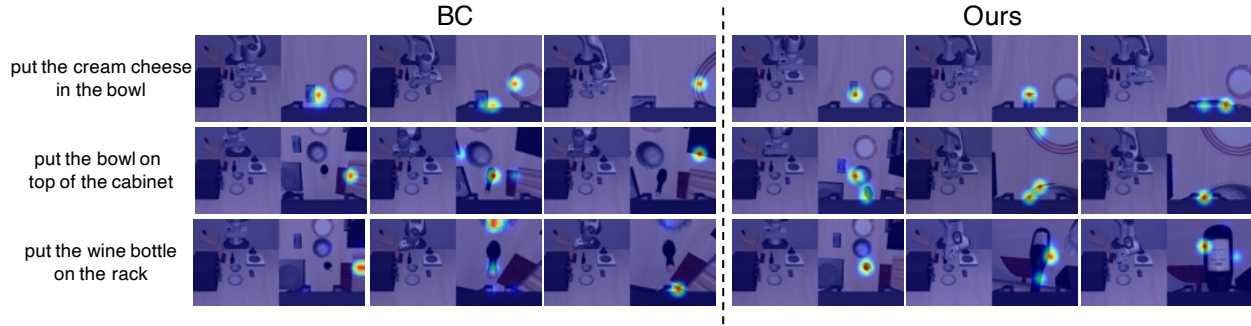


Figure 7. The attention maps of BC and Ours in spatial transformer. We extract the attention weights between spatial CLS token and RGB tokens, highlighting the policy’s focus on specific spatial regions during decision-making. The heatmaps reveal our policy’s targeted attention on task-relevant areas, in contrast to BC’s tendency to focus on irrelevant backgrounds. This underscores the effectiveness of input tracks in the spatial transformer as good task prompts, guiding the CLS token to attend to appropriate areas.

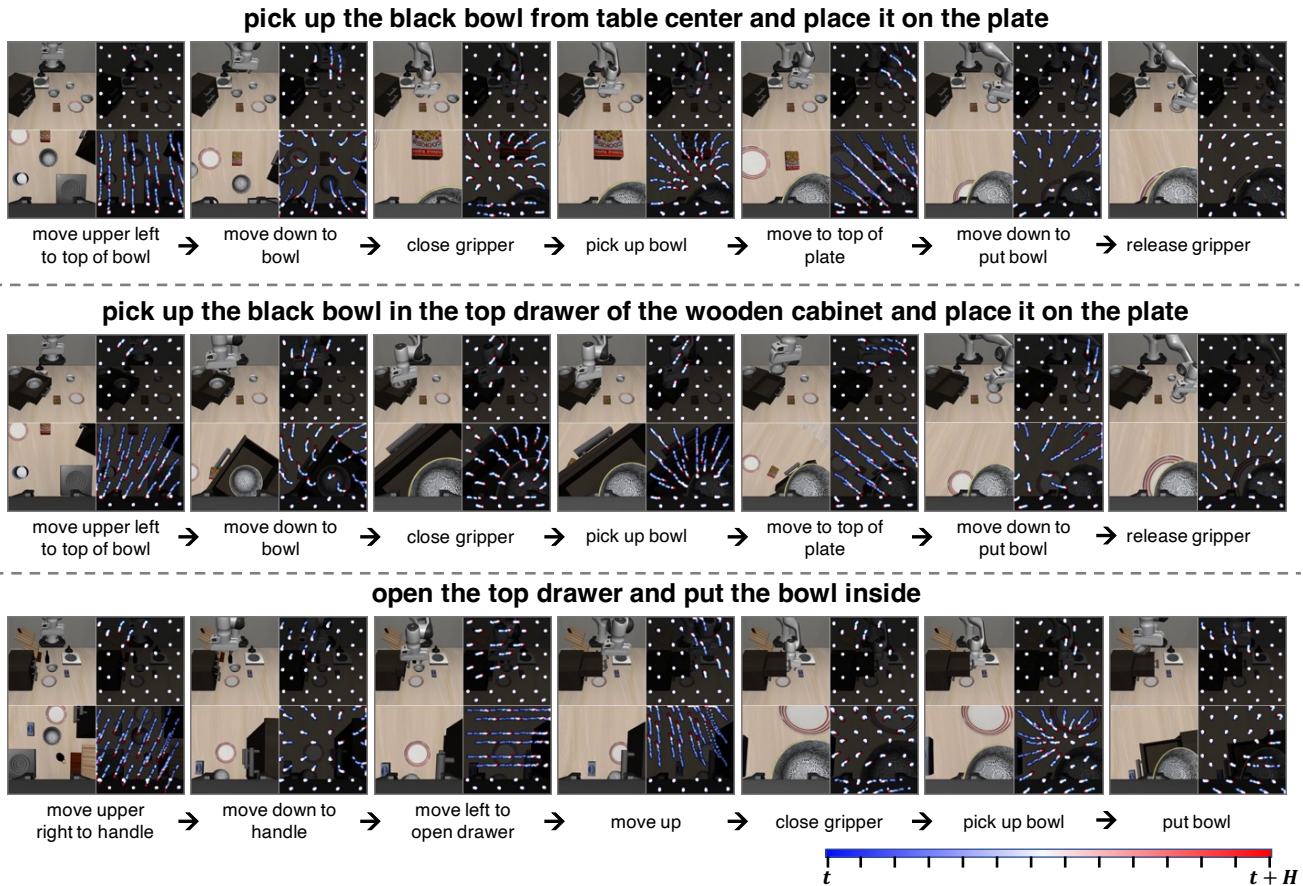


Figure 8. We visualize the predicted tracks during online rollout in these three example tasks. Each subfigure includes a title of the benchmark’s language description to define the task goal, base-view and wrist-view images with corresponding tracks, and our annotations detailing key events (not model inputs). We can see that predicted tracks align with language instructions throughout the process. It decomposes the high-level task goal into fine-grained subgoals at each timestep. And the policy correctly follows the subgoals, leading to the successful completion of the tasks.

hope to scale up our work to more diverse video datasets. Additionally, even after we have pre-trained a track model,

currently we are still relying on action-labeled demonstration data to learn the control policies. In the future, we hope

to extend our work to reinforcement learning settings where no additional demonstrations are needed in policy learning.

## 8. Acknowledgement

This work was supported in part by the BAIR Industrial Consortium, and the InnoHK of the Government of the Hong Kong Special Administrative Region via the Hong Kong Centre for Logistics Robotics. This work is also supported by the Ministry of Science and Technology of the People’s Republic of China, the 2030 Innovation Megaprojects “Program on New Generation Artificial Intelligence” (Grant No. 2021AAA0150000), and the National Key R&D Program of China (2022ZD0161700). This work is done when Chuan Wen is visiting UC Berkeley.

## References

- [1] A Pedro Aguiar and Joao P Hespanha. Trajectory-tracking and path-following of underactuated autonomous vehicles with parametric modeling uncertainty. *IEEE transactions on automatic control*, 52(8):1362–1379, 2007. 2
- [2] Bowen Baker, Ilge Akkaya, Peter Zhokov, Joost Huizinga, Jie Tang, Adrien Ecoffet, Brandon Houghton, Raul Sampedro, and Jeff Clune. Video pretraining (vpt): Learning to act by watching unlabeled online videos. *Advances in Neural Information Processing Systems*, 35:24639–24654, 2022. 3, 6, A1
- [3] Homanga Bharadhwaj, Abhinav Gupta, Shubham Tulsiani, and Vikash Kumar. Zero-shot robot manipulation from passive human videos. *arXiv preprint arXiv:2302.02011*, 2023. 3
- [4] Kevin Black, Mitsuhiro Nakamoto, Pranav Atreya, Homer Walke, Chelsea Finn, Aviral Kumar, and Sergey Levine. Zero-shot robotic manipulation with pretrained image-editing diffusion models. *arXiv preprint arXiv:2310.10639*, 2023. 2, 3, 6, A1, A2
- [5] Anthony Brohan, Noah Brown, Justice Carbajal, Yevgen Chebotar, Joseph Dabis, Chelsea Finn, Keerthana Gopalakrishnan, Karol Hausman, Alex Herzog, Jasmine Hsu, et al. Rt-1: Robotics transformer for real-world control at scale. *arXiv preprint arXiv:2212.06817*, 2022. 2
- [6] Tom Brown, Benjamin Mann, Nick Ryder, Melanie Subbiah, Jared D Kaplan, Prafulla Dhariwal, Arvind Neelakantan, Pranav Shyam, Girish Sastry, Amanda Askell, et al. Language models are few-shot learners. In *Neural Information Processing Systems (NeurIPS)*, 2020. 2
- [7] Pim De Haan, Dinesh Jayaraman, and Sergey Levine. Causal confusion in imitation learning. *Advances in Neural Information Processing Systems*, 32, 2019. A3
- [8] Jacob Devlin, Ming-Wei Chang, Kenton Lee, and Kristina Toutanova. BERT: Pre-training of deep bidirectional transformers for language understanding. In *Proceedings of the 2019 Conference of the North American Chapter of the Association for Computational Linguistics: Human Language Technologies, Volume 1 (Long and Short Papers)*, pages 4171–4186, Minneapolis, Minnesota, 2019. Association for Computational Linguistics. 4, 6
- [9] Carl Doersch, Ankush Gupta, Larisa Markeeva, Adrià Re-casens, Lucas Smaira, Yusuf Aytar, João Carreira, Andrew Zisserman, and Yi Yang. Tap-vid: A benchmark for tracking any point in a video, 2023. 3
- [10] Carl Doersch, Yi Yang, Mel Vecerik, Dilara Gokay, Ankush Gupta, Yusuf Aytar, Joao Carreira, and Andrew Zisserman. Tapir: Tracking any point with per-frame initialization and temporal refinement, 2023. 3
- [11] Yilun Du, Sherry Yang, Bo Dai, Hanjun Dai, Ofir Nachum, Joshua B Tenenbaum, Dale Schuurmans, and Pieter Abbeel. Learning universal policies via text-guided video generation. In *Thirty-seventh Conference on Neural Information Processing Systems*, 2023. 2, 3, 6, A1
- [12] Alejandro Escontrela, Ademi Adeniji, Wilson Yan, Ajay Jain, Xue Bin Peng, Ken Goldberg, Youngwoon Lee, Danijar Hafner, and Pieter Abbeel. Video prediction models as rewards for reinforcement learning. *Neural Information Processing Systems*, 2023. 2, 3
- [13] Hao-Shu Fang, Hongjie Fang, Zhenyu Tang, Jirong Liu, Chenxi Wang, Junbo Wang, Haoyi Zhu, and Cewu Lu. Rh20t: A comprehensive robotic dataset for learning diverse skills in one-shot. In *Towards Generalist Robots: Learning Paradigms for Scalable Skill Acquisition@ CoRL2023*, 2023. 2
- [14] Ankit Goyal, Arsalan Mousavian, Chris Paxton, Yu-Wei Chao, Brian Okorn, Jia Deng, and Dieter Fox. Ifor: Iterative flow minimization for robotic object rearrangement. In *Proceedings of the IEEE/CVF Conference on Computer Vision and Pattern Recognition*, pages 14787–14797, 2022. 2
- [15] Jiayuan Gu, Sean Kirmani, Paul Wohlhart, Yao Lu, Montserrat Gonzalez Arenas, Kanishka Rao, Wenhao Yu, Chuyuan Fu, Keerthana Gopalakrishnan, Zhuo Xu, et al. Rt-trajectory: Robotic task generalization via hindsight trajectory sketches. *arXiv preprint arXiv:2311.01977*, 2023. 2
- [16] Kaiming He, Xinlei Chen, Saining Xie, Yanghao Li, Piotr Dollár, and Ross Girshick. Masked autoencoders are scalable vision learners. In *Proceedings of the IEEE/CVF conference on computer vision and pattern recognition*, pages 16000–16009, 2022. 4
- [17] Zixuan Huang, Xingyu Lin, and David Held. Mesh-based dynamics model with occlusion reasoning for cloth manipulation. In *Robotics: Science and Systems (RSS)*, 2022. 2
- [18] Nikita Karaev, Ignacio Rocco, Benjamin Graham, Natalia Neverova, Andrea Vedaldi, and Christian Rupprecht. Co-tracker: It is better to track together. *arXiv:2307.07635*, 2023. 2, 3, A3
- [19] Wonjae Kim, Bokyung Son, and Ildoo Kim. Vilt: Vision-and-language transformer without convolution or region supervision, 2021. 5, A2
- [20] Alexander Kirillov, Eric Mintun, Nikhila Ravi, Hanzi Mao, Chloe Rolland, Laura Gustafson, Tete Xiao, Spencer Whitehead, Alexander C Berg, Wan-Yen Lo, et al. Segment anything. In *IEEE International Conference on Computer Vision (ICCV)*, 2023. 2
- [21] Po-Chen Ko, Jiayuan Mao, Yilun Du, Shao-Hua Sun, and Joshua B Tenenbaum. Learning to Act from Actionless Video through Dense Correspondences. *arXiv:2310.08576*, 2023. 3, 6, A1

- [22] Yunzhu Li, Shuang Li, Vincent Sitzmann, Pulkit Agrawal, and Antonio Torralba. 3d neural scene representations for visuomotor control. *arXiv preprint arXiv:2107.04004*, 2021. 2
- [23] Xingyu Lin, Yufei Wang, Zixuan Huang, and David Held. Learning visible connectivity dynamics for cloth smoothing. In *Conference on Robot Learning*, 2021. 2
- [24] Xingyu Lin, John So, Sashwat Mahalingam, Fangchen Liu, and Pieter Abbeel. Spawnnnet: Learning generalizable visuomotor skills from pre-trained networks, 2023. 5
- [25] Bo Liu, Yifeng Zhu, Chongkai Gao, Yihao Feng, Yuke Zhu, Peter Stone, et al. Libero: Benchmarking knowledge transfer for lifelong robot learning. In *Thirty-seventh Conference on Neural Information Processing Systems Datasets and Benchmarks Track*, 2023. 2, 5, A2, A3
- [26] Yecheng Jason Ma, Shagun Sodhani, Dinesh Jayaraman, Osbert Bastani, Vikash Kumar, and Amy Zhang. VIP: Towards universal visual reward and representation via value-implicit pre-training. In *The Eleventh International Conference on Learning Representations*, 2023. 3
- [27] Ajay Mandolekar, Danfei Xu, Josiah Wong, Soroush Nasiriany, Chen Wang, Rohun Kulkarni, Li Fei-Fei, Silvio Savarese, Yuke Zhu, and Roberto Martín-Martín. What matters in learning from offline human demonstrations for robot manipulation. *arXiv preprint arXiv:2108.03298*, 2021. 2
- [28] Lucas Manuelli, Yunzhu Li, Pete Florence, and Russ Tedrake. Keypoints into the future: Self-supervised correspondence in model-based reinforcement learning, 2020. 2
- [29] Suraj Nair, Aravind Rajeswaran, Vikash Kumar, Chelsea Finn, and Abhinav Gupta. R3m: A universal visual representation for robot manipulation. In *Conference on Robot Learning*, pages 892–909. PMLR, 2023. 2, 3, 6, A1
- [30] Abhishek Padalkar, Acorn Pooley, Ajinkya Jain, Alex Bewley, Alex Herzog, Alex Irpan, Alexander Khazatsky, Anant Rai, Anikait Singh, Anthony Brohan, et al. Open x-embodiment: Robotic learning datasets and rt-x models. *arXiv preprint arXiv:2310.08864*, 2023. 2
- [31] Xue Bin Peng, Pieter Abbeel, Sergey Levine, and Michiel Van de Panne. Deepmimic: Example-guided deep reinforcement learning of physics-based character skills. *ACM Transactions On Graphics (TOG)*, 37(4):1–14, 2018. 2
- [32] Zengyi Qin, Kuan Fang, Yuke Zhu, Li Fei-Fei, and Silvio Savarese. Keto: Learning keypoint representations for tool manipulation. In *2020 IEEE International Conference on Robotics and Automation (ICRA)*, pages 7278–7285. IEEE, 2020. 2
- [33] Adam Rashid, Satvik Sharma, Chung Min Kim, Justin Kerr, Lawrence Yunliang Chen, Angjoo Kanazawa, and Ken Goldberg. Language embedded radiance fields for zero-shot task-oriented grasping. In *Conference on Robot Learning*, pages 178–200. PMLR, 2023. 2
- [34] Scott Reed, Konrad Zolna, Emilio Parisotto, Sergio Gomez Colmenarejo, Alexander Novikov, Gabriel Barth-Maron, Mai Gimenez, Yury Sulsky, Jackie Kay, Jost Tobias Springenberg, et al. A generalist agent. *arXiv preprint arXiv:2205.06175*, 2022. 2
- [35] Karl Schmeckpeper, Annie Xie, Oleh Rybkin, Stephen Tian, Kostas Daniilidis, Sergey Levine, and Chelsea Finn. Learning predictive models from observation and interaction, 2019. 3
- [36] Daniel Seita, Yufei Wang, Sarthak J Shetty, Edward Yao Li, Zackory Erickson, and David Held. Toolflownet: Robotic manipulation with tools via predicting tool flow from point clouds. In *Conference on Robot Learning*, pages 1038–1049. PMLR, 2023. 2
- [37] Younggyo Seo, Kimin Lee, Stephen James, and Pieter Abbeel. Reinforcement learning with action-free pre-training from videos, 2022. 2
- [38] Pierre Sermanet, Corey Lynch, Yevgen Chebotar, Jasmine Hsu, Eric Jang, Stefan Schaal, Sergey Levine, and Google Brain. Time-contrastive networks: Self-supervised learning from video. In *2018 IEEE international conference on robotics and automation (ICRA)*, pages 1134–1141. IEEE, 2018. 3
- [39] Pierre Sermanet, Corey Lynch, Yevgen Chebotar, Jasmine Hsu, Eric Jang, Stefan Schaal, Sergey Levine, and Google Brain. Time-contrastive networks: Self-supervised learning from video. In *2018 IEEE international conference on robotics and automation (ICRA)*, pages 1134–1141. IEEE, 2018. 2
- [40] Faraz Torabi, Garrett Warnell, and Peter Stone. Behavioral cloning from observation, 2018. 3
- [41] Mel Vecerik, Carl Doersch, Yi Yang, Todor Davchev, Yusuf Aytar, Guangyao Zhou, Raia Hadsell, Lourdes Agapito, and Jon Scholz. Robotap: Tracking arbitrary points for few-shot visual imitation. *arXiv*, 2023. 3, 5
- [42] Homer Rich Walke, Kevin Black, Tony Z Zhao, Quan Vuong, Chongyi Zheng, Philippe Hansen-Estruch, Andre Wang He, Vivek Myers, Moo Jin Kim, Max Du, et al. Bridgedata v2: A dataset for robot learning at scale. In *Conference on Robot Learning*, pages 1723–1736. PMLR, 2023. 2
- [43] Qianqian Wang, Yen-Yu Chang, Ruojin Cai, Zhengqi Li, Bharath Hariharan, Aleksander Holynski, and Noah Snavely. Tracking everything everywhere all at once, 2023. 3
- [44] Chuan Wen, Jierui Lin, Trevor Darrell, Dinesh Jayaraman, and Yang Gao. Fighting copycat agents in behavioral cloning from observation histories. *Advances in Neural Information Processing Systems*, 33:2564–2575, 2020. A3
- [45] Chuan Wen, Jianing Qian, Jierui Lin, Jiaye Teng, Dinesh Jayaraman, and Yang Gao. Fighting fire with fire: Avoiding dnn shortcuts through priming. In *International Conference on Machine Learning*, pages 23723–23750. PMLR, 2022. A3
- [46] Philipp Wu, Yide Shentu, Zhongke Yi, Xingyu Lin, and Pieter Abbeel. Gello: A general, low-cost, and intuitive teleoperation framework for robot manipulators. *arXiv preprint arXiv:2309.13037*, 2023. 2
- [47] Mengjiao Yang, Yilun Du, Kamyar Ghasemipour, Jonathan Tompson, Dale Schuurmans, and Pieter Abbeel. Learning interactive real-world simulators. *arXiv preprint arXiv:2310.06114*, 2023. 2, 3
- [48] Tianhao Zhang, Zoe McCarthy, Owen Jow, Dennis Lee, Xi Chen, Ken Goldberg, and Pieter Abbeel. Deep imitation

learning for complex manipulation tasks from virtual reality teleoperation. In *2018 IEEE International Conference on Robotics and Automation (ICRA)*, pages 5628–5635. IEEE, 2018. 2

# Appendix

## Table of Contents

---

<b>A Additional Experimental Results</b>	<b>A1</b>
A.1 Numerical Results . . . . .	A1
A.2 Comparisons to Variations of the UniPi Baseline . . . . .	A1
<b>B Detailed Policy Architecture</b>	<b>A2</b>
<b>C Implementation and Experimental Details</b>	<b>A3</b>
C.1 Track Filtering for Track Transformer Training . . . . .	A3
C.2 Training Details . . . . .	A3

---

## A. Additional Experimental Results

### A.1. Numerical Results

We report the numeric values for Figure 4 in Table 3. All methods use 20% of the demonstration trajectories except the oracle. See Sec. A.2 for details about the comparisons on UniPi and UniPi-Replan.

Table 3. Average success rate on LIBERO benchmark. Our method performs consistently better than all the baselines across all suites. UniPi-Replan is only evaluated for a single seed due to the computation cost.

Method	Libero-Spatial	Libero-Object	Libero-Goal	Libero-Long	Libero-90
BC-Full-Trainset (Oracle)	71.83 ± 3.70	71.00 ± 7.97	76.33 ± 1.31	24.17 ± 2.59	-
BC	39.00 ± 8.20	51.83 ± 13.54	42.50 ± 4.95	16.67 ± 3.66	29.78 ± 1.14
R3M-finetune [29]	49.17 ± 3.79	52.83 ± 2.25	5.33 ± 1.43	9.17 ± 2.66	9.59 ± 0.27
VPT [2]	37.83 ± 4.29	19.50 ± 0.82	3.33 ± 2.36	3.83 ± 1.65	-
UniPi [11, 21]	<b>69.17 ± 3.75</b>	59.83 ± 3.01	11.83 ± 2.02	5.83 ± 2.08	-
UniPi-Replan [4]	-	31.00	3.00	-	-
Ours	68.50 ± 1.78	<b>68.00 ± 6.18</b>	<b>77.83 ± 0.82</b>	<b>39.33 ± 15.80</b>	<b>48.41 ± 2.09</b>

### A.2. Comparisons to Variations of the UniPi Baseline

UniPi [11] proposes to train a language-conditioned video diffusion model  $f_\theta$  during video pre-training. During policy learning, given the initial image observation  $o_0$  and the language  $l$ , UniPi first generates all future frames  $\tilde{o}_1, \dots, \tilde{o}_{T-1} = f_\theta(o_0, l)$  and then learns an inverse dynamics model that predicts the action at each time step  $a_t = \pi(o_t, \tilde{o}_{t+1})$ . UniPi then executes the actions open-loop. However, training a diffusion model to predict the full video can be computation intensive, As such, the UniPi implementation in our paper follows the one in Ko et al. [21], where we predict  $N = 7$  future frames as the sub-goals for the policy, denoted as  $\tilde{o}_1, \dots, \tilde{o}_N$ . During training, we evenly sample  $N$  frames in an episode for training the video prediction model. During policy learning, we train a goal-conditioned policy  $\pi(a_t, \text{done}|o_t, \tilde{o}_i)$ , where  $i \in 1, \dots, N$  is the image sub-goal and  $t$  denotes the current timestep. The policy additionally predicts a done flag to determine when it should switch from the current sub-goal  $\tilde{o}_i$  to the next sub-goal  $\tilde{o}_{i+1}$ . ATM’s superiority over UniPi can be attributed to two reasons. First, ATM uses a more structured sub-goal representation of point trajectories. Second, ATM performs closed-loop inference, proposing a new sub-goal at each time step, while UniPi’s video diffusion process is too slow to be referenced at every time step.

To train the UniPi policy, we sample  $o_i$  from a future frame  $o_t$  where  $t \in [t, t + t_{max}]$ . We choose  $t_{max}$  for each task suite ( $t_{max} = 16$  for LIBERO-Object and LIBERO-Spatial,  $t_{max} = 50$  for LIBERO-Goal and LIBERO-Long). To mitigate

dataset imbalance when learning the done flag, we sample  $o_i$  as the next frame 10% of the time. We perform MSE regression on both the action  $a_t$  and done.

In order to decouple the two advantages of ATM over UniPi additionally compare with a UniPi variation where we train the video prediction model to predict a fixed time step into the future  $\tilde{o}_{t+H} = f_{\theta}(o_t)$  for every  $H$  steps of policy execution, where  $H = 8$ . As this variation replans the sub-goal more frequently, we call this method *UniPi-Replan*, similar to the implementation in [4]. The results are shown in Table 3. Surprisingly, we found that this variation performs even worse than UniPi. **We thus draw the conclusion that a structured sub-goal representation can be much more effective than an image sub-goal.** The reason is that predicting an image goal at a fixed future time step can be a difficult objective for the video prediction model, leading to inconsistent subgoals. Please refer to the failure videos of various baselines on our website. Additionally, this method requires heavy computation. A comparison of the computation needed is shown in Table 4. Due to the computation cost, we only evaluate UniPi-Replan on LIBERO-Object and LIBERO-Goal and report the average success across 10 trials on one policy seed.

Table 4. Computation cost for performing a single task consisting of 600 time steps for different methods. ATM performs trajectory generation at each time step while being computationally efficient. UniPi performs an open-loop future goal generation once at the beginning using a video diffusion model. UniPi-Replan generates image sub-goals at more frequent time steps and is the slowest.

Method	ATM	UniPi	UniPi-Replan
Computation (TFLOPS)	1.56	39.29	2946.75

## B. Detailed Policy Architecture

We include a more detailed visual of the ViT-T [19, 25] policy used in our experiments in Figure 9. The input to our policy is a set of temporally stacked images across multiple views  $o_t \in \mathbb{R}^{V \times T \times C \times H \times W}$ , and proprioception  $p_t \in \mathbb{R}^{D_p}$ . To process these inputs, ViT-T consists of three stages:

**Spatial Encoding:** We encode all modalities at each timestep. We first leverage the frozen track transformer to propose a set of tracks as described in Section 4.1 for all  $V$  frames in  $o_t$ . We then project each modality with modality-specific encoders into a shared embedding space  $\mathbb{R}^D$ . Each modality’s tokens are embedded using a shared learned modality token, and modality-specific positional embeddings. We then concatenate tokens across all modalities and views with a learned spatial CLS token, and perform self-attention on the sequence. We extract the spatial CLS token as the representation.

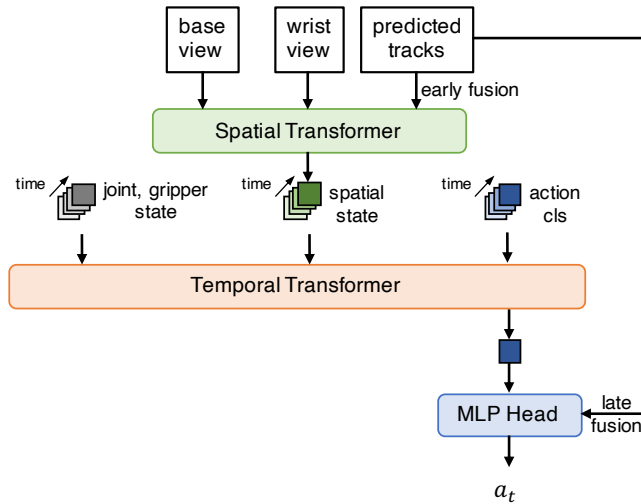


Figure 9. To summarize spatial information, we perform self-attention on a sequence consisting of all views’ track and image patches and a CLS token. To integrate information across time, we perform casual self-attention between spatial CLS token, proprioception, and an action CLS token per timestep. To regress actions, we concatenate each timestep’s action CLS token and proposed tracks.

**Temporal Decoding:** We process the encoded modalities across timesteps into actions. We first project the proprioception at each timestep into the same shared embedding space  $\mathbb{R}^D$ . We then interleave the encoded proprioception, the spatial CLS token, and a learned action CLS token across timesteps into a sequence, before performing causally-masked self attention between the sequence.

**Action Head:** We treat each timestep’s output independently and parameterize actions using an MLP. For each timestep, we take the action CLS token, and fuse the CLS token with the reconstructed tracks of the current timestep.

## C. Implementation and Experimental Details

### C.1. Track Filtering for Track Transformer Training

As introduced in Section 4.1, we adopt a heuristic to filter out the static points in the background and then utilize an off-the-shelf tracking model to generate the corresponding tracks of the large-motion points. The visualization of the sampled points before and after the filtering process is shown in Figure 10.



Figure 10. Given a video (left), we query 1000 randomly sampled points using an off-the-shelf TAP model (middle), where each colored dot represents the starting position of a track. We then filter the tracks using a heuristic of their position displacement across the video and re-sample about these points (right). From observation, the extracted tracks are concentrated around informative objects, such as robot’s gripper and manipulation targets.

### C.2. Training Details

We list the training hyperparameters for the track transformer and track-guided policy in Table 5 and 6, which are fixed for all experiments in Section 5. We train all models on 4 A100 GPUs with DeepSpeed strategy.

We train the track transformer using the ground truth tracks generated by CoTracker [18] and save the checkpoint with the lowest validation loss as our final model to apply for policy learning. We do not incorporate frame stacking for track transformer to avoid the copycat problem (or named causal confusion) [7, 44, 45].

We train policies using the expert demonstrations provided by LIBERO, which is collected by human experts through teleoperation with 3Dconnexion Spacemouse [25]. Since the validation loss in behavioral cloning is not always reliable, we save the checkpoint of the last epoch for online rollout evaluation.

Table 5. Hyperparameters of track transformer training.

Hyperparameters	Track Transformer
epoch	100
batch size	1024
optimizer	AdamW
learning rate	1e-4
weight decay	1e-4
lr scheduler	Cosine
lr warm up	5
clip grad	10
point sampling	variance filtering
number of points	32
track length	16
track patch size	4
image mask ratio	0.5
augmentation	ColorJitter,RandomShift

Table 6. Hyperparameters of policy training.

Hyperparameters	Policy
epoch	100
batch size	512
optimizer	AdamW
learning rate	5e-4
weight decay	1e-4
lr scheduler	Cosine
lr warm up	0
clip grad	100
point sampling	grid
number of points	32
track length	16
frame stack	10
augmentation	ColorJitter,RandomShift